Stochastic Resonance in Neurobiology

David Lyttle

May 2008

Abstract

Stochastic resonance is a nonlinear phenomenon in which the activity of a dynamical system becomes more closely correlated with a periodic input signal in the presence of an optimal level of noise. The first section of this paper provides a definition and mathematical characterization of stochastic resonance, illustrating the phenomenon with classic examples. This is followed by a discussion of how stochastic resonance can be found in simple mathematical models of single neurons, as illustrated by numerical investigations. Finally an overview of experimental studies in which stochastic resonance has been observed in real biological neurons is provided.

1 Stochastic Resonance: Definition and Examples

1.1 Definition and History

Stochastic resonance is a phenomenon in which the behavior of a system in a noisy environment becomes more sensitive to an external periodic stimulus at some optimal finite level of noise intensity. This can be considered somewhat counterintuitive, in that noise, which is often thought of as a nuisance, in this setting actually plays a constructive role in signal detection. Despite this counterintuitive nature however, stochastic resonance has been demonstrated experimentally in a wide variety of settings. Most notably for the purposes of this paper, stochastic resonance has been demonstrated in both theoretical models of neurons as well as actual biological neurons.

The first appearance of stochastic resonance in the literature was a paper by Benzi et al. in 1981, in which it was proposed as a means of explaining the periodic recurrence of ice ages [13]. Statistical analysis of geophysical data indicated that the glacial-interglacial transitions occur with an average periodicity of about 100,000 years. Furthermore, there exists an eccentricity in the Earth's orbit, which causes small periodic fluctuations in the amount of energy received by the earth from the sun. The periodicity of this fluctuation has a time scale that roughly coincides with the glaciation cycles. What Benzi et al. proposed was that climactic noise, i.e. the random, small time-scale fluctuations in the earth's climate, make it possible for this small periodic perturbation in received energy to manifest itself in the form of periodic glaciation cycles. The proposed mechanism by which this can occur was termed stochastic resonance [13].

While the Benzi group's conclusions regarding the periodicity of the ice ages is still subject to debate, the general mechanism of stochastic resonance has since appeared in other contexts. After the initial ideas were published, the field was largely quiescent until 1989, when McNamara et al. demonstrated experimentally the presence of stochastic resonance in a bistable ring laser[3]. Then in 1993, in an experiment to be described in some detail later in this paper, stochastic resonance was demonstrated in crayfish sensory neurons by Douglass et al. [9]. This, coupled with the development of a more general characterization of stochastic resonance as a threshold phenomenon independent of dynamics, led to a widespread interest in applications of the idea to biological systems in general, and neuroscience in particular [14].

1.2 Classical SR

In its classical setting, stochastic resonance applies to bistable nonlinear dynamical systems subject to noise and periodic forcing. A generic form of these these types of systems is the following [10]:

$$\frac{dx}{dt} = -\frac{dV}{dx} + \epsilon \cos(\omega_0 t + \varphi) + \xi(t) \tag{1}$$

Here $x(t)$ is the state variable corresponding to the position of a particle in a potential, and $V(x)$ is a double-well potential in which two stable equilibria are separated by an unstable equilibrium resting atop a potential barrier. The difference between the maximum and the two minima is given by the barrier height $V_0 = \frac{a^2}{4b}$. The periodic forcing term is given by $\epsilon \cos(\omega_0 t + \varphi)$ while $\xi(t)$ represents the additive noise.

To understand what stochastic resonance is and how it can arise in this type of system, it is perhaps best to consider a particular canonical example, first put forth by McNamara et. al [12], which has been cited repeatedly in the literature. In this example, $V(x)$ is a symmetric, bistable potential well given by

$$V(x) = -\frac{a}{2}x^2 + \frac{b}{4}x^4 \tag{2}$$

This has two stable equilibria at $x_\pm = \pm c = \pm\sqrt{\frac{a}{b}}$ when $\epsilon = 0$,and an unstable equilibrium at x=0 lying between the two. Furthermore in this system V_0 is the height f the potential when $\epsilon = 0$, while $V_1 = \epsilon c$ is the amplitude of the modulation in barrier height when the periodic forcing is turned on. $\xi(t)$ refers to zero mean, Gaussian white noise with intensity D and autocorrelation function:

$$< \xi(t)\xi(0) >= 2D\delta(t) \tag{3}$$

For simplicity, let $\varphi = 0$. The effect of the periodic forcing, then, is to successively raise and then lower the potential barriers of the right and left wells in turn. This process is illustrated by Figure 1 (from Gammaitoni et al.) [10]:

Figure 1: Periodic modulation of a symmetric double well (Gammaittoni et. al) [10]

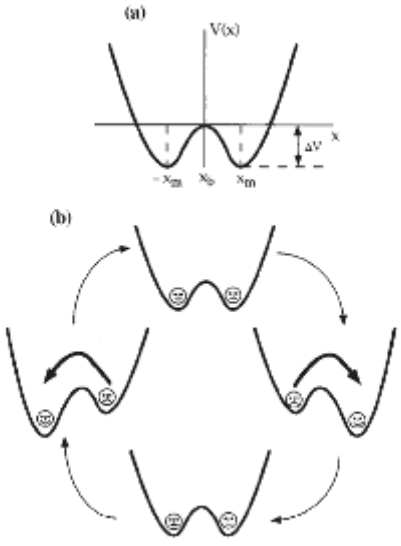

With no periodic forcing, i.e. when ϵ = 0, The behavior of the system will consist of x(t) fluctuating around the minima with a variance proportional to D, and occasionally making random noise-induced

hops from one well to the other. According to McNamara, in the limit when D is much smaller than V_0, the mean first passage time is given by the Kramers time [12]:

$$r_K = \frac{2\pi e^{2V_0/D}}{[V''(0)V''(c)]^{1/2}} = \frac{\sqrt{2}\pi}{a} e^{-\frac{V_0}{D}} \tag{4}$$

The introduction of periodic forcing causes a periodic biasing of one well over the other, which induces the transition probability densities for escaping each well to vary periodically in time. This continuous system can be analyzed in a variety of sophisticated ways, such as numerically solving the associated Fokker-Plank equation, and a thorough review of these methods is given in Gammaitonni et al. [10]. However a more analytically tractable approach is given in McNamara et al. and involves reducing the system to a discrete, two state approximation [12]. This approximation ignores the intrawell dynamics, and considers only whether the particle in is one well or the other, where each state corresponds to the minima $x_\pm$. The relevant dynamics of the system is then reduced to a series of jumps from one well to the other. The starting point for this approximation is given by the master equation:

$$\dot{n}_\pm(t) = -R_\mp n_\pm + R_\pm n_\mp \tag{5}$$

where $n_+(t)$ and n_- are the probabilities that the particle is in the well corresponding to x_+ or x_-, respectively, and $R_\pm$ are the transition rates out of the respective states. By utilizing the normalization constraint that $n_+ + n_- = 1$, one can reformulate the master equation as:

$$\dot{n}_\pm(t) = -[R_\mp + R_\pm]n_\pm + R_\pm \tag{6}$$

This can be solved explicitly, with the solution given by:

$$n_\pm = g(t)\left[n_\pm(t_0) + \int_{t_0}^{t} R_\pm(\tau) g^{-1}(\tau) d\tau\right] \tag{7}$$

where

$$g(t) = e^{\left(-\int_{t_0}^{t}[R_+(\tau)+R_-(\tau)]d\tau\right)} \tag{8}$$

Now in general, $R_\pm$ will be in form such that the above integrals cannot be computed explicitly. However, following McNamara [12], this paper will assume that the escape rates take the form:

$$R_\pm = \frac{a}{\sqrt{2}\pi} e^{-2(V_0 \pm V_1 \cos\omega_0 t)/D} \tag{9}$$

For this assumption to be valid, The probability density within a well must be close to equillibrium. This can only hold if signal frequency is slower than the rate at which the probability equillibriates within the well. This is influenced by the curvature at the well minimum $V''(\pm c) = 2a$. Hence the approximation is only valid for $\omega_0 << 2a$.

From this assumption, one can expand $R_\pm$ in terms of the small parameter $\frac{\epsilon c}{D}\cos\omega_0 t$:

$$R_\pm = \frac{1}{2}(\alpha_0 \mp \alpha_1 \frac{\epsilon c}{D}\cos\omega_0 t + \alpha_2 (\frac{\epsilon c}{D})^2 \cos^2\omega_0 t \mp ...), \tag{10}$$

which leads to:

$$R_+(t) + R_-(t) = \alpha_0 + \alpha_2 (\frac{\epsilon c}{D})^2 \cos^2\omega_0 t + ... \tag{11}$$

where

$$\frac{1}{2}\alpha_0 = \frac{a}{\sqrt{2}\pi} e^{-2(V_0/D)} \tag{12}$$

and

$$\frac{1}{2}\alpha_1 = \frac{\sqrt{2}a}{\pi}e^{-2(V_0/D)} = 2\alpha_0 \tag{13}$$

etc.

This expansion now allows for the computation of the following first order approximation of the integral in Equation 8:

$$n_+(t\left|x_0,t_0\right.) = \left(e^{-\alpha_0(t-t_0)}\left(2\overline{\delta_{x_0,c}} - 1 - \frac{\alpha_1\frac{\epsilon c}{D}\cos\omega_0 t_0 + \phi}{(\alpha_0^2+\omega_0^2)^{1/2}}\right) + 1 + \frac{\alpha_1\frac{\epsilon c}{D}\cos\omega_0 t + \phi}{(\alpha_0^2+\omega_0^2)^{1/2}}\right) \tag{14}$$

where $\phi = \arctan\frac{\omega_0}{\alpha_0}$. Note that here that $\overline{\delta_{x_0,c}}$ is 1 if the particle is initially in the + state at time $t = t_0$ and zero if it starts out in the - state. The expression $n_+(t\,|x_0,t_0)$ denotes the conditional probability that $x(t)$ is in the + state at time t given that the state at time t_0 was x_0 (note that $n_-(t\,|x_0,t_0)$ is defined similarly, except it concerns the - state). From the expression it is now possible to calculate the various statistical properties of the system, including the autocorrelation function, which becomes

$$< x(t)x(t+\tau) >= lim_{t_0\to\infty} < x(t)x(t+\tau)\,|x_0,t_0 > \tag{15}$$

$$= c^2e^{-\alpha_0|\tau|}\left(1 - \frac{\alpha_1^2(\frac{\epsilon c}{D})^2\cos^2\omega_0 t_0 + \phi}{(\alpha_0^2+\omega_0^2)}\right) + \frac{c^2\alpha_1^2(\frac{\epsilon c}{D})^2[\cos\omega_0\tau + cos[\omega_0(2t+\tau)+2\phi]]}{2(\alpha_0^2+\omega_0^2)} \tag{16}$$

Now, by taking the Fourier transform of the time average of the autocorrelation function, one can compute the power spectrum:

$$< S(\Omega) >_t = \frac{\omega_0}{2\pi}\int_{-\infty}^{\infty} << x(t)x(t+\tau) >>_t e^{-i\Omega\tau}d\tau \tag{17}$$

where $<< x(t)x(t+\tau) >>_t$ is the time average of the autocorrelation function. This yields

$$< S(\Omega) >_t = \left(1 - \frac{\alpha_1^2(\frac{\epsilon c}{D})^2}{2(\alpha_0^2+\omega_0^2)}\right)\left(\frac{2c^2\alpha_0}{\alpha_0^2+\Omega^2}\right) + \left(\frac{\pi c^2\alpha_1^2(\frac{\epsilon c}{D})^2}{2(\alpha_0^2+\omega_0^2)}\right)[\delta(\Omega-\omega_0)+\delta(\Omega-\omega_0)] \tag{18}$$

Note that it is sufficient for the purposes of this example to consider only the one-sided average power spectrum (for $\Omega > 0$ only). Taking this into account, and plugging in for α_0 and α_1, the power spectrum can be re-written as

$$S(\Omega) = \left(1 - \frac{\frac{4a^2\epsilon^2}{\pi^2D^2}e^{-4V_0/D}}{\frac{2a^2}{\pi^2}e^{-4V_0/D}+\omega_0^2}\right)\left(\frac{\frac{4\sqrt{2}ac^2}{\pi}e^{-2V_0/D}}{\frac{2a^2}{\pi^2}e^{-4V_0/D}+\omega_0^2}\right) + \left(\frac{\frac{8a^2\epsilon^2}{\pi^2D^2}e^{-4V_0/D}}{\frac{2a^2}{\pi^2}e^{-4V_0/D}+\omega_0^2}\right)\delta(\Omega-\omega_0) \tag{19}$$

Here the signal output corresponds to the second term and the noise output is given by the first. From the above one can derive the signal to noise ratio (SNR):

$$SNR = \left(\frac{\sqrt{2}a\epsilon^2c^2}{D^2}e^{-2V_0/D}\right)\times\left(1 - \left(\frac{\frac{4a^2\epsilon^2}{\pi^2D^2}e^{-4V_0/D}}{\frac{2a^2}{\pi^2}e^{-4V_0/D}+\omega_0^2}\right)\right)^{-1} \tag{20}$$

It is worthwhile to pause at this point and inspect the influence of various parameters upon the above two equations. As can be observed, ϵ serves to strengthen increase the signal portion of the output in each equation. V_0 and a have slightly more complicated effects, in that they affect the geometry of the wells and hence the escape rates out of each wells. However this construction is sufficiently general to allow for the stochastic resonance effects described below across a wide range of values of V_0 and

a. Of real interest is the impact of the parameter D, the noise term, which has a more subtle effect to be described shortly. Note that the second factor in the above expression is the fraction of the total power resulting from the noise, with the part subtracted from 1 representing the coherent (non-noisy) output. Since typically the signal only makes up a small fraction of the total power, the SNR can be approximated by:

$$SNR \approx \frac{\sqrt{2}a\epsilon^2 c^2}{D^2} e^{-2V_0/D} \tag{21}$$

Inspection of the above expression yields the central result of this analysis. This can be observed by noting that for very small values of D compared to V_0, $e^{-2V_0/D}$ decays faster than D^2 and so $SNR \to 0$. On the other hand, for large values of D, $e^{-2V_0/D}$ approaches 1 but the $\frac{1}{D^2}$ term causes the SNR to go to zero. Consequently, for some intermediate value of D, the SNR must possess a local maximum. Thus the SNR will have a local maximum at some finite, nonzero noise level, which is the key characteristic indicative of stochastic resonance. Furthermore, McNamera et. al provide several arguments as to why this discrete caricature closely approximates the the dynamics of a large class of continuous bistable systems, and support their arguments with numerical simulations [12].

1.3 Threshold or non-dynamical SR

Figure 2: An example of a threshold system displaying stochastic resonance (Gingl et al.) [15]

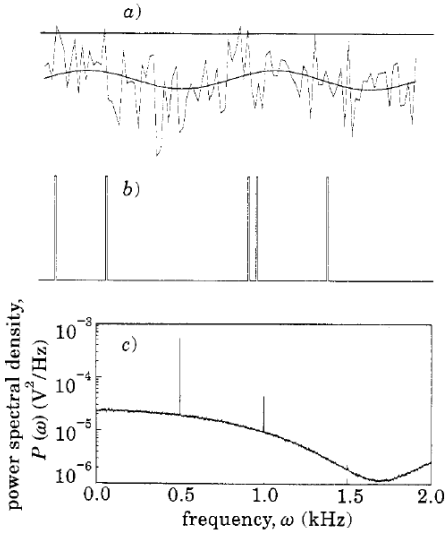

More recently, in 1994-1995, a simpler, and more general characterization of stochastic resonance emerged, which did not require a bistable dynamical system [15, 14]. In this context, the only necessary components for stochastic resonance are some form of threshold, a sub threshold periodic signal, and a source of noise, either intrinsic to the system or added to the signal. An example of such a threshold system is presented in Figure 2, from Gingl et. al [15]. The setup is simple. A threshold value is set, and a subthreshold signal with added noise is presented (see part a of the figure for an example). Each time the noisy signal crosses the pre-defined threshold, an impulse, or 'spike' is recorded (as shown in part b). Part c of the figure demonstrated the power spectrum computed from the resulting train of spikes. This system was demonstrated to exhibit stochastic resonance in that the amplitude of the peak of the power spectum goes through a maximum as a function of the noise intensity [15]. This observation widely extended the class of systems in which stochastic resonance could be expected to be found. In particular, many models of neural activity, which are typically not bistable systems of the form discussed previously, became relevant systems in which to look for stochastic resonance in that they oftentimes

do exhibit threshold-like dynamics. As can be seen, in this system the relevant aspects of the output are the statistical properties of the spike train rather than the dynamical behavior occurring below the the threshold, hence this form of stochastic resonance is referred to as 'non-dynamical' stochastic resonance. The 'resonance' in this case then refers to the extent to which the distribution of spikes is correlated with the signal frequency.

1.4 Measures of Stochastic Resonance

An important consideration in stochastic resonance research is how to quantitatively demonstrate the presence of stochastic resonance effects in the system being studied. Over the years a number of quantitative measures have been used. A common measure, as exemplified in the aforementioned example of a symmetric bistable potential, is the signal-to-noise ratio, or SNR. In essence, the SNR provides a measure of the relative contributions to the total power of a response from its signal and noise components. The power spectrum of a response, which in the presence of a periodic signal can be decomposed into a sum of signal and noise contributions, will in general provide the necessary information for the calculation of the SNR. Alternately, stochastic resonance can be observed directly from the power spectrum, in that the amplitude of the spike corresponding to the periodic component of the response increases, undergoes a maximum, and then decays as a function of noise intensity [10].

A second measure of stochastic resonance that is often used in neuroscience applications is the residence time probability distribution, familiar to experimental biologists as the interspike interval histogram. In the context of the bistable system example, in the absence of periodic forcing, the time spent in one of the attraction basins is a random variable with a probability distribution that decays exponentially with time. Alternately, the same characterization can be given to the time between threshold crossing events in the context non-dynamical stochastic resonance . When periodic forcing is introduced, the distribution resolves to a sequence of exponentially decreasing Gaussian-like peaks. Narrower, higher amplitude first-order peaks indicate the phase synchronization of the switching or threshold-crossing events with the periodic stimulus, and hence SR is present when these peaks go though a maximum as a function of time [10, 11, 14].

2 Applications to Neuroscience

2.1 A Brief Overview of Neuron Structure and Function

Having discussed the central ideas of stochastic resonance, it is now possible to address the implications of the idea to the field of neuroscience. This requires some familiarity with the properties of neurons and in particular the notion of an action potential. Neurons are electrically excitable cells that process and transmit information in the nervous system. The basic gross anatomy of a neuron is as follows:

- The *soma*, the central body of the cell containing the nucleus.
- *Dendrites*, which are heavily branched extensions from the soma that receive the majority of the input to the cell.
- A (usually) single *axon*. The axon extends out from the soma and can possess many branches allowing it to provide input several cells. At the end of the axon is the axon terminal, which contains synaptic vesicles that when stimulated by an action potential release neurotransmitters in order to communicate with target cells. The part of the axon where it emerges from the soma is called the axon hillock, and contains a high concentration of voltage gated ion channels making it the primary region of the neuron in which action potentials are generated. In some neurons the axon is protected by an insulating sheath of myelin that enhances the conduction of action potentials.

The electrical activity of neurons is governed by flows of various ions across the neural membrane. The relevant ions include sodium (Na^+), potassium (K^+), calcium (Ca^{2+}), and chloride (Cl^-). Ions travel across the cell membrane under the influence of forces such as diffusion, active transport, and electric fields. Diffusion results in the net flow of ions from regions of high to low concentrations. However this flow results in a voltage that counteracts the motion of the ions. The fact that the membrane itself is relatively impermeable to ions means that ions must pass through various types of ion channels in order to traverse the membrane. These ion channels can be either open or closed and their state can be regulated by factors such as membrane voltage or the binding of various ligands such as neurotransmitters. Furthermore, neurons possess ion pumps, which serve to maintain specific ion concentrations inside and outside of the cell via the ATP driven active transport of ions across the membrane.

Each species of ion has its own characteristic equilibrium potential, and when that potential is reached, the net flow of ions across the membrane will cease. For a given ion species, the equilibrium potential is given by the Nernst equation:

$$E = \frac{RT}{nF} \ln \frac{[ion]_{outside}}{[ion]_{inside}} \quad (22)$$

where R is the molar gas constant, n is the charge valence of the ion, T is the temperature in Kelvins, and F is the Faraday, i.e. the total charge of one mole of electrons. Furthermore, there exists a voltage at which the net flow across the cell membrane of all ions is zero, this is given by the Goldman equation for the three ions most important to action potential generation:

$$E = \frac{RT}{F} \ln \left(\frac{[K^+]_{out} + [Na^+]_{out} + [Cl^-]_{in}}{[K^+]_{in} + [Na^+]_{in} + [Cl^-]_{out}} \right) \quad (23)$$

In general, the equilibrium potential of human neurons tends to lie in the vicinity of -70 mV. The membrane voltage of a neuron is obviously not always at equilibrium, in fact, the movement of only a few ions can result in a dramatic change in membrane voltage. A sufficiently strong depolarization of the membrane can result in an action potential. The basic mechanism of an action potential (for a given patch of membrane) is as follows:

- In the stimulation/rising phase, a stimulus occurs that depolarizes the membrane at some point, for example, the injection of extra sodium cations into the cell. If this is small, the outward potassium current will overwhelm the influx of sodium and the cell will repolarize back to equilibrium. However if the stimulus is sufficiently strong (a typical threshold value is -45 mV), this depolarization will result in the opening of voltage-gated sodium channels, resulting in even more sodium ions entering the cell, which in turn activated more voltage-gated sodium channels, in a positive-feedback loop. This results in the rapid spike in membrane voltage.

- In the peak/falling phase, the sodium channels become maximally open and then begin to deactivate, reducing sodium permeability. In addition, the spike in voltage results in the opening of voltage-gated potassium channels, allowing potassium to flow out of the cell. The combination of these two process caused the membrane voltage to fall back down toward equilibrium.

- In the hyperpolarization or undershoot phase, the slow closing of the opened potassium channels causes the membrane voltage to fall lower than the equilibrium potential, resulting in an undershoot effect. In a short time, however, the voltage climbs back up to equilibrium.

- In some cases the opened sodium and potassium channels require time to recover before they can be re-opened, resulting in a refractory period in which no new action potentials can occur.

An action potential is typically initiated in the axon hillock, and can travel down the axon as a wave of excitation. The arrival of an action potential at the axon terminal then results in the exocytosis of synaptic vesicles which releasing neurotransmitters into synapses, thus sending a signal to target cells.

Many mathematical models of varying degrees of complexity and biological plausibility have been proposed to capture various aspects of this process. One of the earliest and most sophisticated is the Hodgkin-Huxley model, which Hodgkin and Huxley proposed in order to explain the ionic mechanism of action potential formation in the giant squid axon. This paper will discuss stochastic resonance effects in two considerably simpler (but less biophysically realistic) models: the Fitzhugh-Nagumo model and the Leaky Integrate-and-Fire model.

2.2 SR in Single Neuron Models

2.2.1 The Leaky-Integrate and Fire Model

The Integrate and Fire model of the neuron is one of the oldest models of neural function. Quite remarkably, it was originally proposed in 1907 by Lapicque [4], long before any real understanding of the physiological basis of neural activity had been developed. It has subsequently been modified to account for 'leaky' or imperfect integration of input current, however the basic form remains largely unchanged. Furthermore, the model is still widely used in neural network simulations due to its simplicity, computational efficiency, and relative effectiveness in describing the important computational properties of neurons [2].

In its deterministic form, the leaky integrate and fire model is described by an ODE that determines the sub-threshold dynamics of the membrane voltage and contains a term for the input current as a function of time, along with a reset rule in which the model will 'spike' and then be reset to the equilibrium potential when the membrane potential reaches a predefined threshold. To include the effect of noise, a noise term is added to the ODE. Thus the integrate and fire neuron with periodic forcing and noise can be written down as:

$$\dot{V(t)} = \frac{1}{C}(\frac{-1}{R}V(t) + q\sin(\omega t + \varphi) + D\xi(t)) \tag{24}$$

If

$$V(t) \geq V_{th} \tag{25}$$

then

$$V(t) \stackrel{reset}{\rightarrow} V(0) \tag{26}$$

Where V is the membrane potential, q, ω, and are the amplitude, frequency, and phase of the periodic forcing, R and C are parameters, and $D\xi(t)$ is Gaussian white noise with intensity D. When V reaches V_{th}, it is reset to $V(0)$. Optionally, one can set V to a predefined spike value V_{spike} immediately after a threshold-crossing, and then reset it to $V(0)$.

For the purposes of demonstrating stochastic resonance in this model, the system was solved numerically for several different noise intensities, with parameters provided in the appendix.

Figure 3: Simulation of the Leaky I and F model for various noise intensities

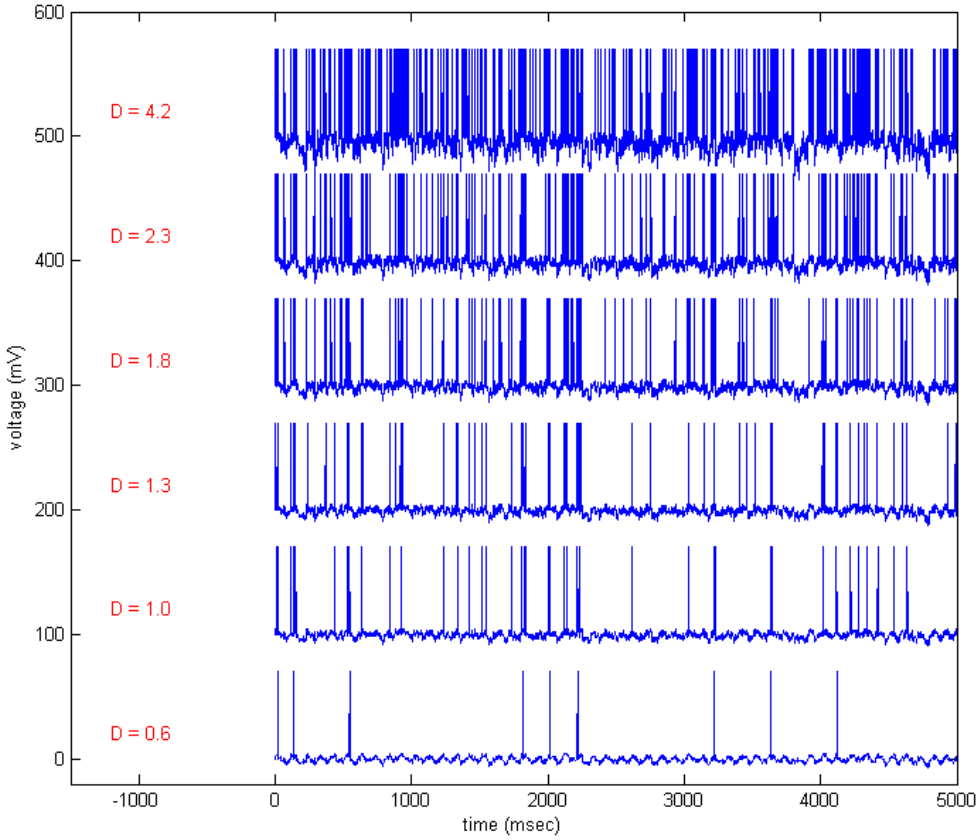

Graphs of several of the solutions can be seen in Figure 3. From visual inspection of the graphs, one can see the signal (as manifest in the output train of spikes) becoming most coherent for an intermediate values, however this alone does not constitute proof of stochastic resonance. Therefore, time-series consisting only of the spike trains with the subthreshold dynamics cut off were generated, and their power spectral densities computed. A graph of three representative power spectra, for low, intermediate, and high values of noise respectively, is provided in Figure 4.

Figure 4: Power spectra for low, medium, and high noise intensities

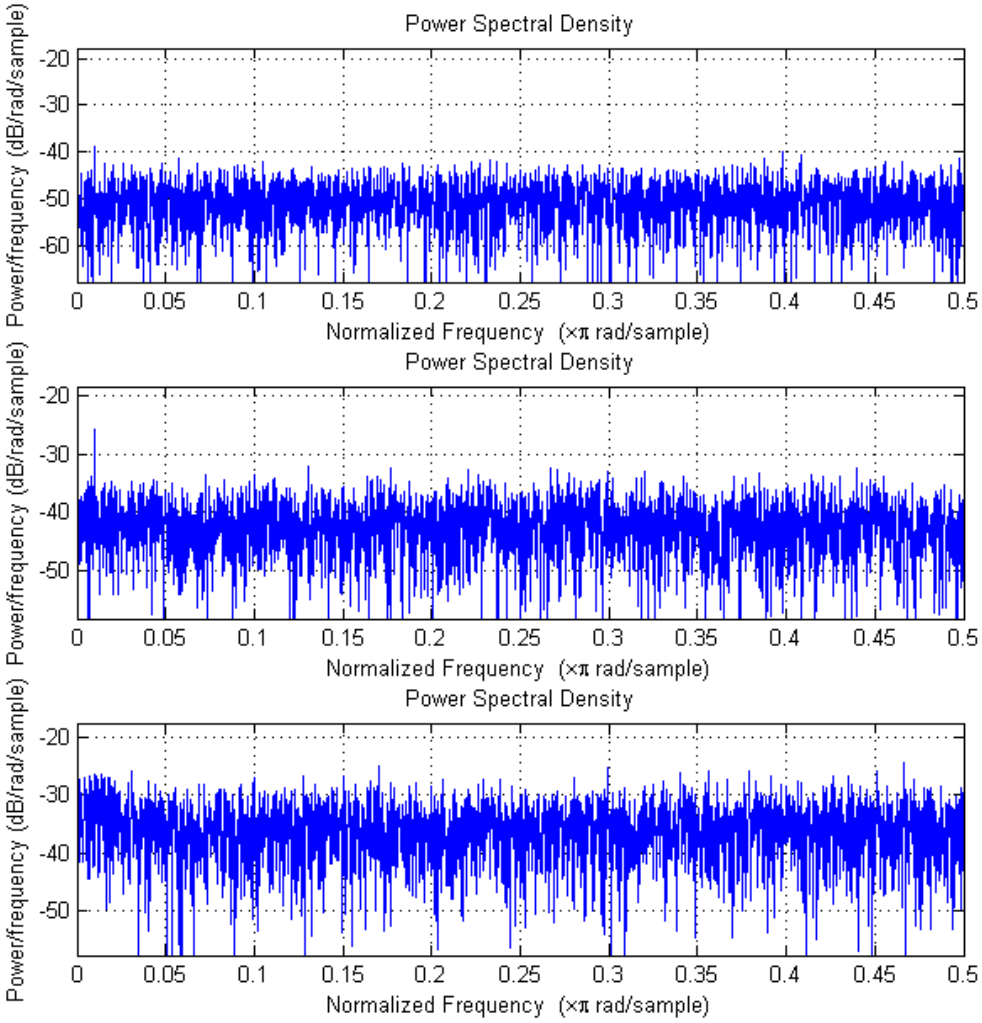

One can observe from the figure a small spike emerging from the noise, at the characteristic frequency of the forcing (around 0.01 on the x-axis). The peak is difficult to discern for low noise values, becomes more pronounced at an intermediate noise value, and then again becomes difficult to discern for high noise values. This is a characteristic signature of stochastic resonance, indicating that the integrate and fire model with noise and periodic forcing is capable of displaying stochastic resonance.

2.2.2 The Fitzhugh-Nagumo Model

The Fitzhugh-Nagumo model was developed by Richard Fitzhugh and Jin-ichi Nagumo in 1961-62 [7]. It is a two dimensional reduction of the Hodgkin-Huxley system given by the equations:

$$\epsilon \dot{v} = v(v-a)(1-v) - w + I \tag{27}$$

$$\dot{w} = v - cw \tag{28}$$

Here v is the voltage-like variable responsible for the fast dynamics (roughly corresponding to the rapid sodium channel activation), while w is the slower recovery-like variable (roughly corresponding to potassium channel activation and sodium channel inactivation). I is the externally applied current, while a and c are parameters, and $\epsilon << 1$ is a small parameter allowing for the separation of time scales. The deterministic Fitzhugh-Nagumo equations display a number of interesting dynamics in their own right. Figure 5 displays the phase plane of the system for a representative set of parameters, with the nullclines and several representative trajectories shown. The basic behaviors of the system that are of interest in this paper are a s follows: When I is given by a pulse of input current exceeds a certain threshold, the system will exhibit an excursion away from equilibrium in phase space, corresponding to a voltage spike. Small input currents result in small-amplitude excursions corresponding to subthreshold oscillations, while large pulses result in large amplitude excursions corresponding to spikes. Furthermore, is a constant level of input current is supplied , the system will exhibit repetitive (tonic) spiking [11, 8].

Figure 5: Phase portrait of the deterministic Fizthugh Nagumo system (Scholarpedia)

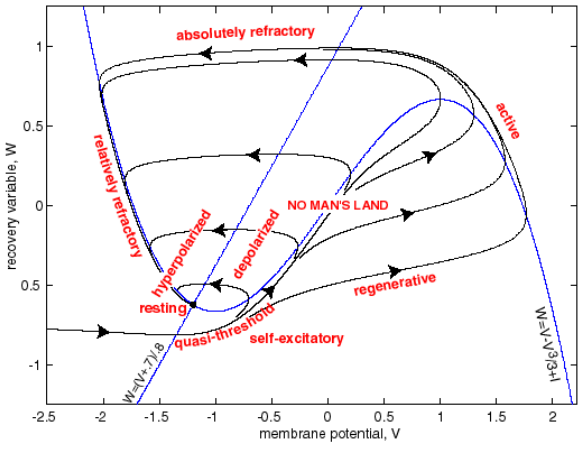

Longtin et. al provide a numerical investigation into stochastic resonance in this model, by using the following set of equations that have been modified to include periodic forcing and noise terms [11]:

$$\epsilon \dot{v} = v(v-a)(1-v) - w + \xi(t) \tag{29}$$

$$\dot{w} = v - cw - [b + r\sin\beta t)] \tag{30}$$

Here the noise term, $\xi(t)$, is given by an Ornstein-Uhlenbeck process with correlation time τ_c and variance $\frac{D}{\tau_c}$. The authors justification for using an Ornstein Uhlenbeck process rather than white noise was that doing so allowed them to control the correlation time τ_c. Hence D can be thought of as the intensity of the noise. A graph of a representative realization of the modified Fitzhugh Nagumo system (shown for the v variable) from Longtin et. al is given in Figure 6 [11]. In the figure the upward peaks are considered action potentials if they exceed 0.5 in amplitude. The researchers generated this example using the parameter values $\beta = 15$, $a = 0.5$, $b = 0.15$, $c = 1.0$, $r = 1$, $\epsilon = 0.005$, $D = 10^{-5}$, and $\tau_c = 0.01$.

Figure 6: A specific realization of the stochastic, periodically forced Fitzhugh-Nagumo system (Longtin et. al) [11]

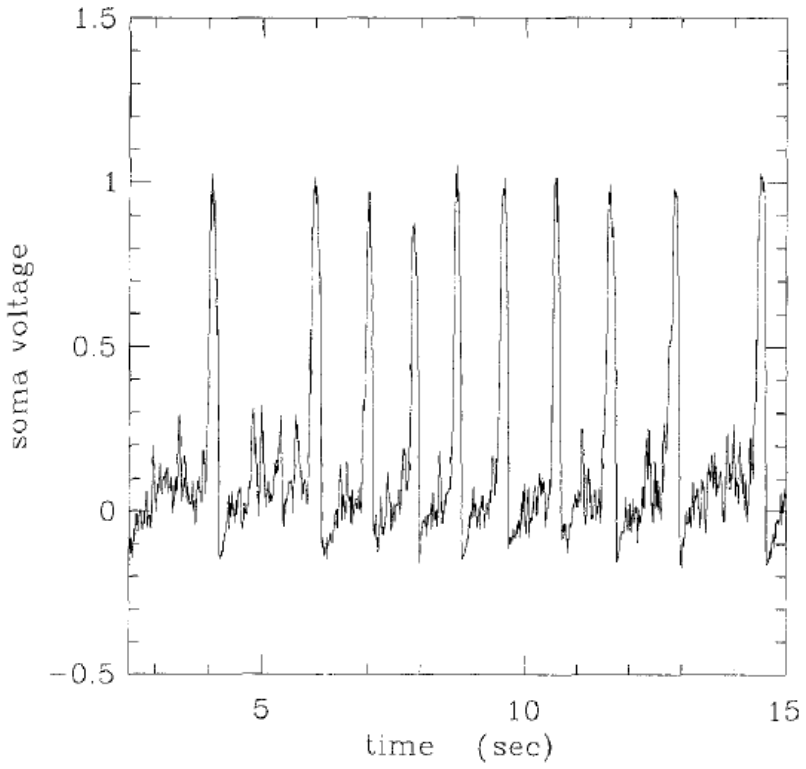

Also in this study, Longtin et. al compute the interspike interval histograms for several values of D. Their results for four representative D values is shown in Figures 7 and 8. As can be seen, the second peak reaches its maximum for an intermediate value of noise, thus demonstrating stochastic resonance in this model [11].

Figure 7: ISIHs of the output for four different noise values (Longtin et. al) [11]

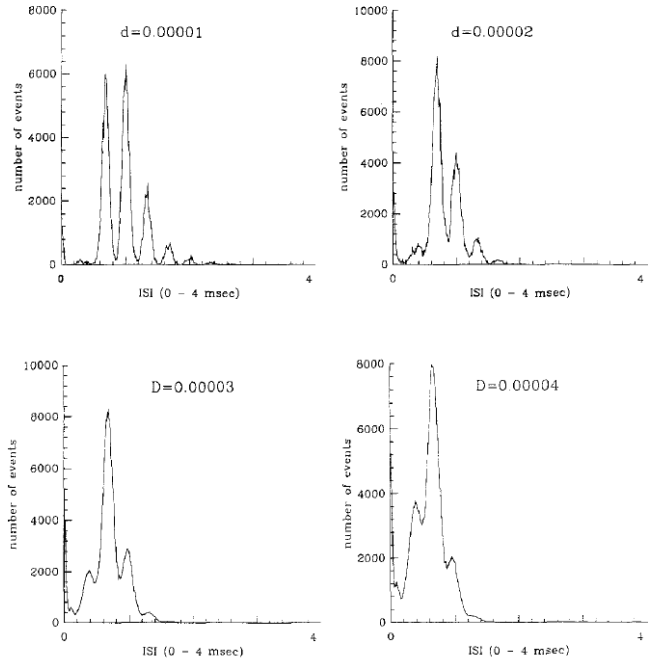

Figure 8: A plot of the heights of the peaks in the ISIHs of the output for different noise values (Longtin et. al) [11]

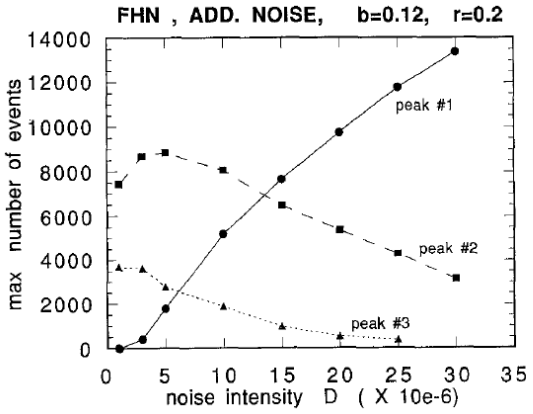

2.3 Experimental Evidence for SR in Neural Systems

2.3.1 SR in Crayfish Mechanosensory Neurons

Given that the phenomenon of stochastic resonance can be observed in simple models of spiking neurons such as the leaky integrate-and-fire model, the obvious question remains as to whether or not real living neurons actually exhibit this property. A key experimental study by Douglass et al. involving crayfish

mechanoreceptors demonstrated that real neurons can in fact display stochastic resonance. Their experiments used near-field mechanoreceptors from the tailfin of the crayfish *Procambarus clarkii*. In these mechanoreceptors, the motion of cuticular hairs triggers electrical activity in the associated nerve roots, which is then propagated as a series of spikes along sensory nerves.

In the experiments, a single crayfish mechanoreceptor hair cell, along with the nerve cord and sixth ganglion, was excised and placed it in crayfish saline. The mechanoreceptor was then mounted vertically on an electromagnetic motion transducer. The transducer was driven by an additive combination of a sinusoidal signal and wide-band Gaussian noise of varying intensities, and extracellular recordings from the nerve root were taken and windowed to isolate spikes from a single cell [9]. These spike trains were then processed to obtain power spectra and interspike interval histograms. Power spectra from a single representative treatment for three different noise intensities are represented in Figure , which was reproduced from Douglass et. al [9].

Figure 9: Power spectra of crayfish spikes for three different noise intensities (Douglass et. al) [9]

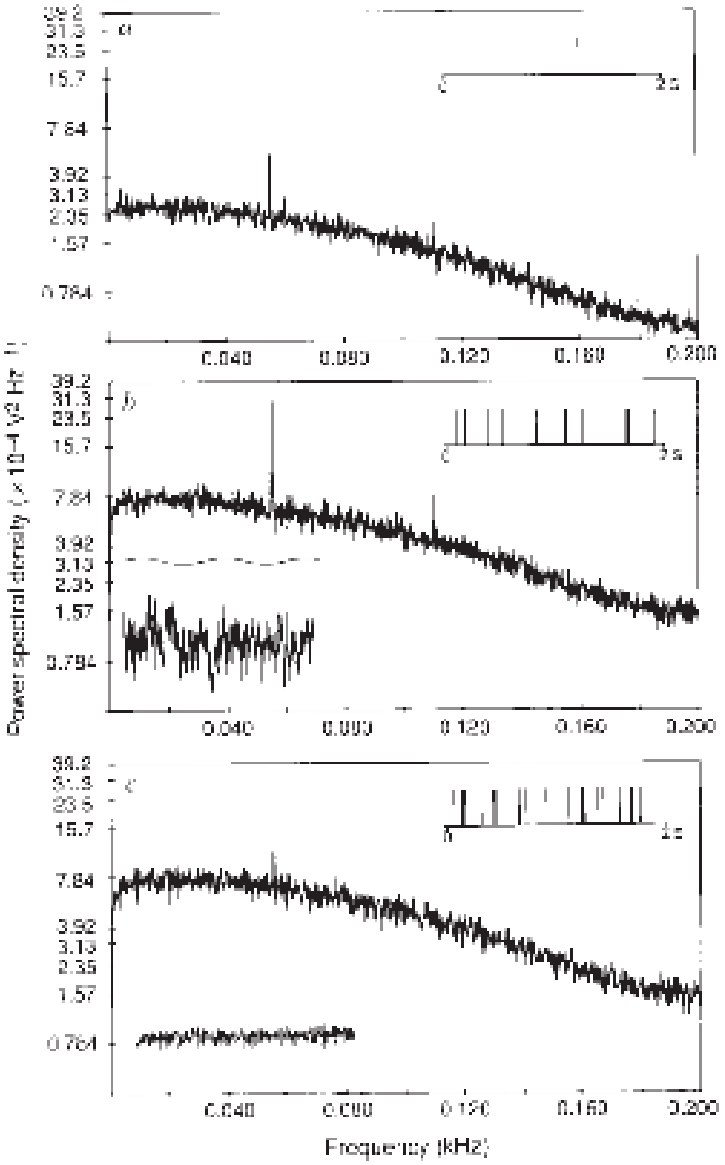

Note that in the bottom left corner of the second and third subfigures are plots of the noise, while the second subfigure also has a plot of the signal. In the upper right corner of each of the subfigures is a plot of the spike train from which the power spectrum was computed. As can be observed from the figure, the peak in the power spectrum corresponding to the signal frequency is small at a low level of noise, becomes larger for an intermediate value of noise, and then decays again at high noise levels. This is a characteristic signature of stochastic resonance, indicating that the phenomenon is in fact a relevant property of crayfish sensory neurons. Researchers have speculated that this may be of use to the crayfish in the context of predator avoidance, in that stochastic resonance could facilitate the detection of periodic currents caused by nearby swimming fish in the presence of background water turbulence [9, 14].

2.3.2 Behavioral SR in Paddlefish

The aforementioned crayfish study, having established that sensory neurons can display stochastic resonance, raises the general question of whether or not animals can in fact make some use of the the enhanced signal detection enabled by stochastic resonance. A study conducted by Russell et. al involving the feeding behavior of paddlefish demonstrated that stochastic resonance can in fact influence animal behavior [5]. Paddlefish live in North American rivers, and feed on a variety of zooplankton, particularly *Daphnia*. Since the muddy turbidity of the waters in which they live inhibits the visual detection of their prey, paddlefish have developed a long, flattened 'rostrum' extending from their mouth that is covered with passive electroreceptors. This rostrum is used to locate plankton such as *Daphnia*, which produce low frequency external fields. As is to be expected, more distant plankton are more difficult to locate. The researchers in this study hypothesized that the presence of background electrical noise at some optimal amplitude might allow paddlefish to locate and capture more distant prey as compared to zero-field controls via the mechanism of stochastic resonance [5].

Figure 10: Experimental setup from the Russell study. (a) depicts the paddlefish in the swim mill, (b) shows the signal emitted from the *Daphnia*, (c) shows the background noise, and (d) is the amplitude spectrum of the applied noise (Russell et. al) [5]

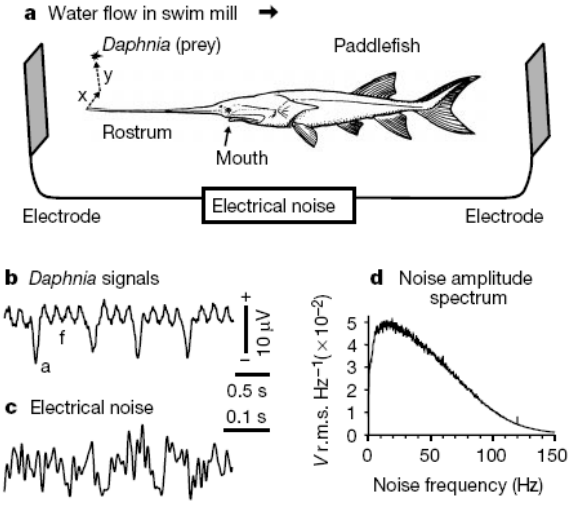

To test their hypothesis, the researchers placed a paddlefish in a recirculating stream of water (a swim mill), along with *Daphnia*. A random electrical stimulus of varying intensity was passed through the water, and the feeding behavior of the paddlefish was recorded via videotape. Analysis of the videotape revealed that the spatial distribution of strike locations was more spread out at a low but nonzero noise amplitude, indicating that stochastic resonance was aiding in the detection of more distant prey.

Figure 11: Spatial distribution of feeding strike locations for three noise intensities(Russell et. al) [5]

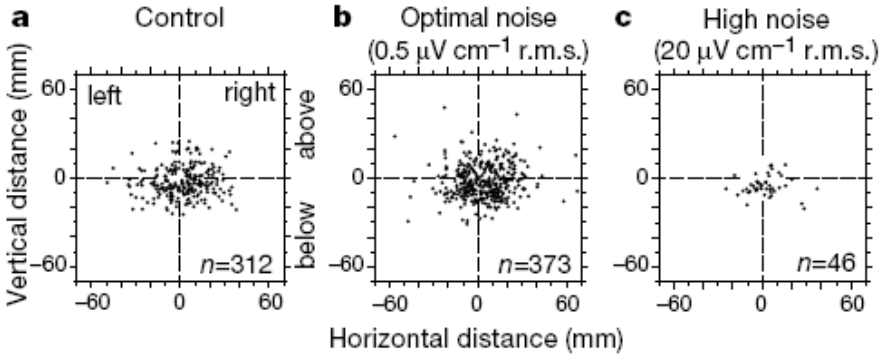

In addition, the researchers demonstrated that swarms of *Daphnia* can serve as a source of electrical noise in nature, and that the noise produced was within the bandwidth of paddlefish electroreceptors. Thus this study provides evidence that stochastic resonance can conceivably play a role in the behavior of animals in nature[5].

3 Conclusions

Given that threshold systems subject to a weak signal with added noise can be found in a wide variety of physical and biological systems, the ubiquitous nature of the stochastic resonance phenomenon should come as no surprise. Furthermore, the presence of stochastic resonance in neural systems, and the fact that it can even influence behavior, opens up a variety of intriguing questions. For example there has been proposals that some organisms might be capable of actually tuning their endogenous noise levels so as to optimize neural computation [14]. However the mechanism by which this could occur remains unclear, so this proposal remains highly speculative. Nonetheless, as research into the stochastic resonance continues, its presence and importance in a wide variety of neurobiological contexts is becoming known. Recently several studies have looked into the role of stochastic resonance in human sensory information properties, as summarized in Moss et al. [6]. There has even been research into possible biomedical applications, such as the use of vibrating shoe insoles to help elderly nursing home patients keep their balance while standing [1]. Thus the ubiquitous and yet counterintuitive nature of stochastic resonance makes it a worthwhile field of inquiry, particularly with respect to the neurosciences.

4 Acknowledgements

The author would like to thank Dr. Herman Flaschka and Dr. Kevin Lin for their assistance, advice, and encouragement regarding this project.

5 Appendix

In Figure 3, each time series was computed with a forward-Euler routine in MATLAB for 5000 time steps. The simulation parameters were: $C = 1$, $R = 10$, $V_{th} = 5$, $V_{spike} = 70$,$q = 0.3$, $\omega = \frac{2\pi}{100}$, and $= 0$.

For Figure 4, the three noise intensities were D = 0.6, 1.4, and 4.2, and each subfigure is a an average of 200 power spectra each resulting from different realization of the simulation.

References

[1] J. Harry L. Lipsitz A. Priplata, J. Niemi and J. Collins. Vibrating insoles and balance control in elederly people. *Lancet*, 362:1123–1124, 2003.

[2] L. F. Abbott. Lapicque's introduction of the integrate-and-fire model neuron (1907). *Brain Research Bulletin*, 50:303–304, 1999.

[3] K. Wiesenfeld B. McNamara and R. Roy. Observation of stochastic resonance in a ring laser. *Phys. Rev. Lett.*, 60:2626–2629, 1988.

[4] Translated by: Nicolas Brunel and Mark C. W. van Rossum. Quantitative investigations of electrical nerve excitation treated as polarization: Louis lapicque 1907. *Biol. Cybern.*, 97(5):341–349, 2007.

[5] L. Wilkens D. Russell and F. Moss. Use of behavioural stochastic resonance by paddle fish for feeding. *Nature*, 402:291–294, November 1999.

[6] L. Ward F. Moss and W. Sannita. Stochastic resonance and sensory information processing, a tutorial and review of application. *Clin. Neurophys.*, 115:267–281, 2004.

[7] R. FitzHugh. Impulses and physiological states in theoretical models of nerve membrane. *Biophysical J*, 1:445–466, 1961.

[8] E. M. Izhikevich. *Dynamical Systems in Neuroscience: The Geometry of Exitability and Bursting*. The MIT Press, Cambridge MA, 2007.

[9] E. Pantazelou J. Douglass, L. Wilkens and F. Moss. Noise enhancement of information transfer in crayfish mechanoreceptors by stochastic resonance. *Nature*, 365:337–340, 1993.

[10] P. Jung L. Gammaitoni, P. Hnggi and F. Marchesoni. Stochastic resonance. *Rev. Mod. Phys.*, 70:223–287, 1998.

[11] A. Longtin. Stochastic resonance in neuron models. *J. Stat. Phys.*, 70:309–327, 1993.

[12] B. McNamara and K. Wiesenfeld. Theory of stochastic resonance. *Phys. Rev. A*, 39:4854–4869, 1989.

[13] A. Sutera R. Benzi and A. Vulpiani. The mechanism of stochastic resonance. *L. Phys. A: Math. Gen.*, 14:L453–L457, 1981.

[14] K. Wiesenfeld and F. Moss. Stochastic resonance and the benefits of noise: from ice ages to crayfish and squids. *Nature*, 373:33–36, 1995.

[15] L. Kiss Z. Gingl and F. Moss. Non-dynamical stochastic resonance: theory and experiments with white and arbitrarily coloured noises. *Europhys. Lett.*, 29, 1995.